Food & Function

Accepted Manuscript

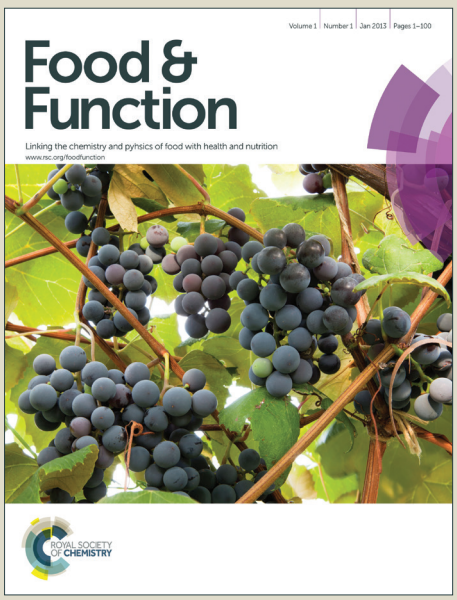

This is an *Accepted Manuscript*, which has been through the Royal Society of Chemistry peer review process and has been accepted for publication.

Accepted Manuscripts are published online shortly after acceptance, before technical editing, formatting and proof reading. Using this free service, authors can make their results available to the community, in citable form, before we publish the edited article. We will replace this *Accepted Manuscript* with the edited and formatted *Advance Article* as soon as it is available.

You can find more information about *Accepted Manuscripts* in the Information for Authors.

Please note that technical editing may introduce minor changes to the text and/or graphics, which may alter content. The journal's standard Terms & Conditions and the Ethical guidelines still apply. In no event shall the Royal Society of Chemistry be held responsible for any errors or omissions in this *Accepted Manuscript* or any consequences arising from the use of any information it contains.

ROYAL SOCIETY OF CHEMISTRY

www.rsc.org/foodfunction

Running title: Grape seed extract and intestinal epithelial health

Grape Seed Extract Improves Epithelial Structure and Suppresses Inflammation in Ileum of IL-10-Deficient Mice

Guan Yang[1], Hui Wang[1],Yifei Kang[1], and Mei-Jun Zhu[1,2]*

[1]School of Food Science, Washington State University, Pullman, WA 99164, USA,

[2]School of Food Science, University of Idaho, Moscow, ID 83844, USA

(*): Corresponding author: Dr. Meijun Zhu, School of Food Science, Washington State University, Pullman, WA 99163 or University of Idaho, Moscow, ID 83844, USA.; Phone: (509) 335-4016; Fax: (509) 335-4815; E-mail: meijun.zhu@wsu.edu

Acknowledgements: This work was financially supported by Washington State University seed grant

Abstract

Defect in intestinal epithelial structure is a critical etiological factor of several intestinal diseases, such as inflammatory bowel disease. The objective of this study was to evaluate the effect of grape seed extract (GSE) which contains a mixture of polyphenols on ileal mucosal structure and inflammation in interleukin (IL)-10-deficient mice, a common model for studying inflammatory bowel disease. Wild-type and IL-10-deficient mice were fed GSE at 0 or 1% (based on dry feed weight) for 16 weeks. The GSE supplementation decreased the crypt depth and increased ($P < 0.05$) the ratio of villus/crypt length in the terminal ileum. Consistently, the dietary GSE decreased ($P < 0.05$) proliferation and enhanced ($P < 0.05$) differentiation of epithelial cells. These changes in gut epithelium were associated with the suppression of nuclear factor kappa-light-chain-enhancer of activated B-cell (NF-κB) signaling. Furthermore, compared with WT mice, IL-10 deletion promoted beclin-1 and AMPK expression, both of which were decreased to normal by GSE supplementation. These changes were associated with alterations in epithelial barrier function as indicated by reduced pore forming claudin-2 protein expression and increased barrier forming claudin-1 protein expression in ileum of GSE supplemented mice. In summary, our data indicates that GSE exerts protective effects to the ileal epithelial structure in IL-10-deficient mice possibly through suppression of inflammatory response.

Keywords: grape seed extract, ileum, tight junction, proliferation, NF-κB, inflammation

INTRODUCTION

Gut epithelial integrity and barrier function are critical for health [1-5]. Because gut epithelium is constantly renewing a balanced epithelial cell proliferation and differentiation is inseparable for its barrier function [6]. Epithelial cells are derived from intestinal stem cells which are located at the bottom of the crypts. These stem cells proliferate and migrate while undergoing differentiation into enterocytes, goblet cells, enteroendocrine cells, and paneth cells [6]. Changes in the rate of cell proliferation and differentiation impair the renewal of intestinal epithelium and integrity [7]. Aberrant cellular proliferation [8, 9] and damaged epithelial barrier integrity are associated with inflammatory bowel diseases (IBD) [10-14]. The identification of factors that prevent mucosal injury and promote proper epithelial development may provide new therapeutic strategies for maintaining intestinal integrity and preventing IBD.

Etiological factors leading to IBD include immunological risk factor, genetic pre-disposition and environmental changes [15, 16]. Though the exact etiology of IBD is far from clear, accumulating evidence points to the importance of environmental factors including dietary bioactive compounds in the incidence of IBD [17-20]. Grape skin and seed extract (GSE) contains a high level of polyphenolic compounds, which are known for their anti-oxidative and anti-inflammatory effects [21-27], and have been widely used as a dietary bioactive compound supplements. GSE supplementation increases intestinal epithelial villus height in pigs [28], reduces the severity of selected disease markers in the proximal colon of DSS-induced colitis in rats [29], and alleviates inflammatory responses in TNBS-induced colitis in rats [30]. GSE has recently been reported to increase occludin and ZO-1 expression in the gut epithelium of rats [31, 32]. In addition, GSE supplementation is recently reported to decrease the symptoms of intestinal mucositis [33, 34].

IL-10-deficient mice (IL10KO) develop spontaneous enterocolitis similar to human Crohn's disease [35], and this model has been widely used for studying gut mucosal inflammation and associated diseases [20, 36, 37]. Recently, our group reported that GSE supplementation ameliorates IBD indices in IL10KO mice, which was associated with decreased inflammatory responses in colonic tissue and alteration in gut microbiota [20]. However, effects of GSE on small intestinal morphology, and epithelial structure and development of IL10KO mice are unknown. The ileum is the most common site for Crohn's disease and its structure and physiology differ from that of the colon. The objective of this study was to evaluate the effects of dietary GSE supplementation on mucosal development in the ileum, and further investigate its protective mechanisms in the ileum of IL10KO mice.

MATERIALS AND METHODS

Grape Seed Extract

GSE (Gravinol-S) was purchased from OptiPure Chemco Industries Inc. (Los Angeles, CA). According to company product specification sheet, it contains a minimum 95% flavonols, of which 82% are oligomeric proanthocyanidins (OPCs), and 12% being the highly active monomeric OPCs. TOF-MS/MS analysis in our lab further indicated that it had catechin monomer 7.3%, dimer 35.8%, trimer 38.6%, tetramer 12.8%, pentamer 5.4%, and trace amount of hexamer.

Animal Care and Experimental Design

C57BL/6 (WT) and IL-10-deficient (IL-10-/-, IL10KO) female mice (Jackson Lab, Bar Harbor, Maine) were housed in temperature-controlled room with a 12 h light and 12 h darkness cycle, with free access to food and water. At 6 weeks of age,

both WT and IL10KO were randomly separated into two groups, and fed either 0 or 1% of GSE (g GSE/g dry food weight) supplemented standard rodent diet for 16 weeks. This resulted in 4 dietary groups: WT-CON, WT-GSE, IL10KO-CON and IL10KO-GSE. Mice were raised in a conventional environment per procedures approved by the Institutional Animal Use and Care Committee of the University of Wyoming. Feed was changed on a daily basis to minimize the oxidation of functional compounds in GSE.

Tissue Collection

On the day of necropsy, mice were anesthetized intraperitoneally with tribromoethanol (250 mg/kg body weight), then killed by cervical dislocation. The ileum section was dissected. A 5 mm segment of terminal ileum was fixed in freshly prepared 4% (w/v) paraformaldehyde (pH7.0), processed, and embedded in paraffin. The remaining ileum tissues were cut open longitudinally, rinsed in PBS, frozen in liquid nitrogen, and stored at -80 °C for further biochemical analyses.

Crypt Depth and Villus Height Measurement

Paraffin embedded ileum tissues were sectioned at 5 μm thickness, deparaffinized and stained with hematoxylin and eosin (H&E) according to a routine protocol. Histological examination and imaging were done under a Lecia DM2000 LED light microscope (200×, Leica Microsystems Inc, Chicago, IL). Villus height and crypt depth were determined by measuring 10 complete villi per image using the Image J 1.30v software (National Institute of Health, USA). At least one image was obtained per section and 5 sections at constant interval (50 μm) were used for taking images.

Goblet Cell Staining

Ileum tissue sections at 5 μm thickness were stained in alcian blue (pH2.5) as previously described [20]. At least one image was obtained per section and 5 sections at constant interval (50 μm) were used for the quantification of goblet cell/total area ratio using the Image J 1.30v software (National Institute of Health, USA).

Epithelial Proliferation Analysis

Proliferation was quantified using proliferation cell nuclear antigen (PCNA) staining as previously reported [38], which labels cells in S- and G1-phases of the cell cycle. Briefly, sections were deparaffinized and hydrated, antigen retrieved and blocked for 30 min in 1.5% goat normal serum and incubated with anti-PCNA antibody (Santa Cruz, 1:800) overnight at 4°C. These sections were then washed with PBST, and signals were visualized with Vectastain ABC and diaminobenzidine kit (Vector Laboratories, Inc., Burlingame, CA), followed by hematoxylin counterstaining. Histological examination was done under a Lecia DM2000 LED light microscope (200×). The total number of PCNA-positive cells per crypt was defined as a mean of proliferating cells in 6-8 sections per sample [38, 39].

Western Blotting

Western blotting analyses were conducted according to previously published procedure [20]. The protein extracts from ileum tissues were separated by 10% SDS-PAGE gels and transferred to nitrocellulose membrane. Antibodies against claudin-1 and claudin-2 were purchased from Invitrogen (Camarillo, CA). Antibodies against phospho-NF-κ B p65 (ser536), NF-κB p65, phospho-AMPK, AMPK and Beclin-1 were purchased from Cell Signaling Technology (Beverly, MA). Anti-GAPDH antibody was purchased from Affinity BioReagents (Golden, CO). Bands were visualized using the ECL chemiluminescence method (GE Healthcare). Band density

was normalized according to the GAPDH content.

Statistical Analysis

Data were analyzed as a complete randomized design using GLM (General Linear Model of Statistical Analysis System, SAS, 2000). Data are expressed as mean ± standard error of the mean (SEM). Mean difference was separated by LSD multiple comparison. Statistical significance is considered as $P <= 0.05$.

RESULTS

Dietary GSE Altered Villus Height and Crypt Depth

There were no difference in body weight and feed intake between genotypes and dietary treatments (Data not shown). No difference was observed for the ileal villus height between all treatment groups (Fig.1). Compared to WT mice, IL10KO mice had numerical higher ileal mucosal length in both CON and GSE fed groups. The GSE supplementation decreased the crypt depth in both WT mice and IL10KO mice, which resulted in increased villus height: crypt depth ratio (Fig. 1).

Dietary GSE Enhanced Goblet Cell Density and Reduced PCNA Staining

Goblet cell is one of the four differentiated epithelial cells and has been used as a marker of cell differentiation [6]. The expression of PCNA correlates with cell proliferation [40]. In the present study, the GSE supplementation increased the density of goblet cells in ileal tissues of both WT and IL10KO mice (Fig. 2), while the PCNA positively labeled cells per crypt were attenuated in IL10KO supplemented with GSE (Fig. 3).

Dietary GSE Suppressed Inflammation and Autophagy

IBD is characterized by chronic inflammation, which is known to induce excessive epithelial proliferation. Indeed, compared to WT mice, the phosphorylation of p65 and total p65, the key mediator of inflammatory NF-κB signaling, were heightened in IL10KO mice (Fig. 4). GSE supplementation significantly decreased NF-κB p65 signaling in IL10KO mice, indicating anti-inflammatory effects of GSE on ileal epithelium in IL10KO mice.

On the other hand, inflammation enhances autophagy, both of which are closely associated with IBD pathogenesis. Consistently, compared to WT mice, the expression of Beclin-1, a key regulator of autophagy, was elevated in IL10KO mice, which was prevented by GSE supplement; no effect of GSE on Beclin-1 expression in WT mice was detected (Fig. 5A). AMP-activated protein kinase (AMPK) is known to induce autophagy. In agreement, AMPK phosphorylation, which is correlated with its activity, was heightened in IL10KO mice compared to that in WT, but restored in GSE supplemented IL10KO mice (Fig. 5B).

Dietary GSE Improved the Expression of Tight Junction Proteins

Epithelial barrier function is a key predisposing factor for IBD, which is affected by inflammation and autophagy. IL10KO mice had numerically lower claudin-1 protein content compared to that in WT (Fig. 6). Claudin-1 protein content in the ileal tissues of IL10KO mice was dramatically increased by GSE supplementation (Fig. 6). On the other hand, the expression of pore forming claudin-2 was reduced in both WT and IL10KO mice supplemented with GSE compared to their respective CON fed mice (Fig. 6). These data suggested the likely improvement of epithelial barrier function by the GSE supplementation.

DISCUSSION

GSE and its constituents have been demonstrated to exert protective roles in various colitis models [29, 41, 42]. Previously, we reported that GSE supplementation exerted favorable effects on colonic tissues, which ameliorated IBD indices in IL10KO mice [20]. The ileum is the most common site for Crohn's disease, and its epithelial structure differs from that of the colon, in this study, the beneficial effect of GSE on the ileal tissues of IL10KO mice was further examined.

GSE supplementation decreased epithelial cell proliferation and increased cell differentiation in the IL10KO mice. These results were in agreement with previous studies showing that GSE decreased cell proliferation in the intestinal tract of APC $^{min/+}$ mice [39] and azoxymethane (AOM)-induced Fischer 344 Rats [43]. Compared to WT mice, IL10KO mice had a numerically increased crypt depth and mucosal length in the ileal tissue, while there was no change observed in villus height between dietary groups within/among genotype. Previous studies showed an increase in crypt cell proliferation and hyperplasia [44] or increased crypt depth in the ileum of mice with DSS-induced colitis[29]; the GSE supplementation reduced crypt depth and decreased mucosal thickness in the terminal ileum of DSS-induced mice [29]. These results are consistent with our observation that GSE supplementation reduced crypt depth and increased villus/crypt ratio in the ileum. The intestine has the ability to compensate epithelial injury through increasing villus height and crypt depth [45]. The observed decrease in crypt depth in IL10KO mice supplemented with GSE might be a beneficial action in response to increased inflammatory responses in the ileal tissues of IL10KO mice.

IBD is characterized with chronic inflammation, which is known to induce aberrant cellular proliferation [8, 9] and damage the epithelial barrier integrity [10-14]. The activation of p65, a key mediator of NF-κB pathway, was elevated in ileum of

IL10CON mice, which was prevented by GSE supplementation. These data are consistent with other reports showing that the GSE supplementation decreased the NF-κB level in rats with AOM-induced aberrant crypt foci [43] and cells with H_2O_2 induced oxidative damage [46], as well as our recent study showing that the GSE supplementation reduced the NF-κB level in the colon of IL10KO mice [20]. The down-regulation of NF-κB activity might partially explain the correction of proliferation, improvement of the differentiation as well as the enhanced expression of tight junction proteins in IL10KO mice supplemented with GSE.

Inflammation is frequently associated with enhanced autophagy. AMPK is known to induce autophagy through direct phosphorylation of Unc-51 like autophagy activating kinase 1 (ULK1) [47]. Consistently, our results showed that both total and phosphorylated AMPK as well as beclin-1 levels were up-regulated in IL10KO mice compared to that of WT mice, which were attenuated by dietary GSE supplementation. An inappropriate activation of autophagy leads to severe mucosal injury and cell death [48, 49], which is known to cause barrier loss [50]. However, recent studies show the beneficial effects of AMPK activation on gut epithelial barrier function. Butyrate [51] and forskolin [52] enhance the intestinal barrier function via AMPK activation *in vitro*, by promoting the formation of tight junction complexes unrelated to cell proliferation and differentiation. In IL10KO mice *in vivo*, enhanced AMPK activity is likely due to the compromised cellular energetics associated with inflammation and aberrant cell proliferation [53]. Thus, dietary GSE suppresses AMPK activity possibly through enhancing cell differentiation and cellular energetics, similar to resveratrol [54].

In summary, our data shows that dietary GSE exerts protective effects to the ileal epithelium of IL10KO mice by restoring a balanced proliferation and differentiation

of epithelial cells, which is likely associated with down-regulation of NF-κB and AMPK activity following GSE supplementation.

References

1. R. J. Hilsden, J. B. Meddings, J. Hardin, D. G. Gall and L. R. Sutherland, *Inflamm Bowel Dis*, 1999, **5**, 85-91.
2. M. Camilleri, K. Madsen, R. Spiller, B. Greenwood-Van Meerveld and G. N. Verne, *Neurogastroenterol Motil*, 2012, **24**, 503-512.
3. K. R. Groschwitz and S. P. Hogan, *J Allergy Clin Immunol*, 2009, **124**, 3-20.
4. L. C. Yu, *Pediatr Neonatol*, 2009, **50**, 247-254.
5. O. Vaarala, *Immunol Cell Biol*, 2012, **90**, 271-276.
6. C. Crosnier, D. Stamataki and J. Lewis, *Nat Rev Genet*, 2006, **7**, 349-359.
7. J. Yang, C. Y. Chan, B. Jiang, X. Yu, G. Z. Zhu, Y. Chen, J. Barnard and W. Mei, *PLoS Genet*, 2009, **5**, e1000363.
8. A. C. Bharti, N. Donato, S. Singh and B. B. Aggarwal, *Blood*, 2003, **101**, 1053-1062.
9. Z. Estrov, S. Shishodia, S. Faderl, D. Harris, Q. Van, H. M. Kantarjian, M. Talpaz and B. B. Aggarwal, *Blood*, 2003, **102**, 987-995.
10. T. Kisseleva, L. Song, M. Vorontchikhina, N. Feirt, J. Kitajewski and C. Schindler, *J Clin Invest*, 2006, **116**, 2955-2963.
11. M. Rotches-Ribalta, C. Andres-Lacueva, R. Estruch, E. Escribano and M. Urpi-Sarda, *Pharmacol Res*, 2012, **66**, 375-382.
12. M. Amasheh, A. Fromm, S. M. Krug, S. Amasheh, S. Andres, M. Zeitz, M. Fromm and J. D. Schulzke, *J Cell Sci*, 2010, **123**, 4145-4155.
13. Y. Zhang and J. Li, *Biochem Biophys Res Commun*, 2012, **428**, 321-326.
14. H. Wang, J. X. Zhao, N. Hu, J. Ren, M. Du and M. J. Zhu, *World J Gastroenterol*, 2012, **18**, 2180-2187.
15. K. J. Maloy and F. Powrie, *Nature*, 2011, **474**, 298-306.
16. M. Scharl and G. Rogler, *Curr Opin Gastroenterol*, 2012, **28**, 301-309.
17. H. Wang, Y. S. Xue, H. Y. Zhang, Y. Huang, G. Yang, M. Du and M. J. Zhu, *Mol Nutr Food Res*, 2013, **57**, 2253-2257.
18. H. Yoon, Y. S. Yoon, M. S. Kim, M. J. Chung and D. Y. Yum, *Toxicol Res*, 2014, **30**, 27-32.
19. L. G. Albenberg, J. D. Lewis and G. D. Wu, *Curr Opin Gastroenterol*, 2012, **28**, 314-320.
20. H. Wang, Y. Xue, H. Zhang, Y. Huang, G. Yang, M. Du and M. J. Zhu, *Mol Nutr Food Res*, 2013, **57**, 2253-2257.
21. M. P. Robich, R. M. Osipov, R. Nezafat, J. Feng, R. T. Clements, C. Bianchi, M. Boodhwani, M. A. Coady, R. J. Laham and F. W. Sellke, *Circulation*, 2010, **122**, S142-149.
22. Q. Chen, E. Wang, L. Ma and P. Zhai, *Lipids Health Dis*, 2012, **11**, 56.
23. J. Tome-Carneiro, M. Gonzalvez, M. Larrosa, M. J. Yanez-Gascon, F. J. Garcia-Almagro, J. A. Ruiz-Ros, M. T. Garcia-Conesa, F. A. Tomas-Barberan and J. C. Espin, *Am J Cardiol*, 2012, **110**, 356-363.
24. K. Szkudelska and T. Szkudelski, *Eur J Pharmacol*, 2010, **635**, 1-8.
25. K. B. Harikumar and B. B. Aggarwal, *Cell Cycle*, 2008, **7**, 1020-1035.
26. S. Hogan, C. Canning, S. Sun, X. Sun, H. Kadouh and K. Zhou, *J Agric Food Chem*, 2011, **59**, 3035-3041.

27. B. T. Metzger, D. M. Barnes and J. D. Reed, *Journal of medicinal food*, 2009, **12**, 854-860.
28. J. Sehm, H. Lindermayer, C. Dummer, D. Treutter and M. W. Pfaffl, *J Anim Physiol Anim Nutr (Berl)*, 2007, **91**, 289-296.
29. K. Y. Cheah, S. E. Bastian, T. M. Acott, S. M. Abimosleh, K. A. Lymn and G. S. Howarth, *Dig Dis Sci*, 2013, **58**, 970-977.
30. Y. H. Wang, B. Ge, X. L. Yang, J. Zhai, L. N. Yang, X. X. Wang, X. Liu, J. C. Shi and Y. J. Wu, *Int Immunopharmacol*, 2011, **11**, 1620-1627.
31. P. Song, R. Zhang, X. Wang, P. He, L. Tan and X. Ma, *J Agric Food Chem*, 2011, **59**, 6227-6232.
32. K. M. Goodrich, G. Fundaro, L. E. Griffin, A. Grant, M. W. Hulver, M. A. Ponder and A. P. Neilson, *Nutr Res*, 2012, **32**, 787-794.
33. K. Y. Cheah, G. S. Howarth and S. E. Bastian, *PLoS One*, 2014, **9**, e85184.
34. K. Y. Cheah, G. S. Howarth, R. Yazbeck, T. H. Wright, E. J. Whitford, C. Payne, R. N. Butler and S. E. Bastian, *Cancer Biol Ther*, 2009, **8**, 382-390.
35. R. Kuhn, J. Lohler, D. Rennick, K. Rajewsky and W. Muller, *Cell*, 1993, **75**, 263-274.
36. A. C. Gomes-Santos, T. G. Moreira, A. B. Castro-Junior, B. C. Horta, L. Lemos, D. N. Cruz, M. A. Guimaraes, D. C. Cara, D. M. McCafferty and A. M. Faria, *Clin Dev Immunol*, 2012, **2012**, 560817.
37. J. Bassaganya-Riera, M. DiGuardo, M. Viladomiu, A. de Horna, S. Sanchez, A. W. Einerhand, L. Sanders and R. Hontecillas, *J Nutr*, 2011, **141**, 1318-1325.
38. Y. Cai, W. Wang, H. Liang, L. Sun, D. H. Teitelbaum and H. Yang, *PLoS One*, 2012, **7**, e44772.
39. B. Velmurugan, R. P. Singh, N. Kaul, R. Agarwal and C. Agarwal, *Neoplasia*, 2010, **12**, 95-102.
40. F. J. Kubben, A. Peeters-Haesevoets, L. G. Engels, C. G. Baeten, B. Schutte, J. W. Arends, R. W. Stockbrugger and G. H. Blijham, *Gut*, 1994, **35**, 530-535.
41. X. L. Li, Y. Q. Cai, H. Qin and Y. J. Wu, *Can J Physiol Pharmacol*, 2008, **86**, 841-849.
42. Y. H. Wang, X. L. Yang, L. Wang, M. X. Cui, Y. Q. Cai, X. L. Li and Y. J. Wu, *Can J Physiol Pharmacol*, 2010, **88**, 888-898.
43. B. Velmurugan, R. P. Singh, R. Agarwal and C. Agarwal, *Mol Carcinog*, 2010, **49**, 641-652.
44. M. S. Geier, C. L. Smith, R. N. Butler and G. S. Howarth, *Dig Dis Sci*, 2009, **54**, 1222-1228.
45. E. Q. Haxhija, H. Yang, A. U. Spencer, X. Sun and D. H. Teitelbaum, *Pediatr Surg Int*, 2007, **23**, 379-390.
46. Z. Jia, Z. Song, Y. Zhao, X. Wang and P. Liu, *Mol Vis*, 2011, **17**, 210-217.
47. J. Kim, M. Kundu, B. Viollet and K. L. Guan, *Nat Cell Biol*, 2011, **13**, 132-141.
48. A. A. Maynard, K. Dvorak, L. Khailova, H. Dobrenen, K. M. Arganbright, M. D. Halpern, A. R. Kurundkar, A. Maheshwari and B. Dvorak, *Am J Physiol Gastrointest Liver Physiol*, 2010, **299**, G614-622.
49. B. Levine and J. Yuan, *J Clin Invest*, 2005, **115**, 2679-2688.
50. A. H. Gitter, F. Wullstein, M. Fromm and J. D. Schulzke, *Gastroenterology*, 2001, **121**, 1320-1328.
51. L. Peng, Z. R. Li, R. S. Green, I. R. Holzman and J. Lin, *J Nutr*, 2009, **139**, 1619-1625.
52. M. Egawa, H. Kamata, A. Kushiyama, H. Sakoda, M. Fujishiro, N. Horike, M. Yoneda, Y. Nakatsu, G. Ying, Z. Jun, Y. Tsuchiya, K. Takata, H. Kurihara and T. Asano, *Placenta*, 2008, **29**, 1003-1008.

53. D. M. Thomson, J. D. Brown, N. Fillmore, S. K. Ellsworth, D. L. Jacobs, W. W. Winder, C. A. Fick and S. E. Gordon, *J Physiol*, 2009, **587**, 2077-2086.
54. V. Desquiret-Dumas, N. Gueguen, G. Leman, S. Baron, V. Nivet-Antoine, S. Chupin, A. Chevrollier, E. Vessieres, A. Ayer, M. Ferre, D. Bonneau, D. Henrion, P. Reynier and V. Procaccio, *J Biol Chem*, 2013, **288**, 36662-36675.

Figure legends

Fig.1. Mucosal thickness, villus height and crypt depth in ileum of IL10KO or WT mice fed a CON (□) or GSE supplemented (■) diet. Histogram bars with the same letter do not differ significantly at $P = 0.05$ (Mean ± SEM, n=8). IL10KO: IL-10-deficient; WT: wild type; CON: control; GSE: grape seed extract.

Fig.2. Goblet cell density in ileum of IL10KO or WT mice fed a CON (□) or GSE supplemented (■) diet. (A) Statistic data; (B) Representative images, original magnification at 200×. Histogram bars with the same letter do not differ significantly at $P = 0.05$ (Mean ± SEM, n=8). The black arrows indicate blue stained goblet cell. IL10KO: IL-10-deficient; WT: wild type; CON: control; GSE: grape seed extract.

Fig.3. PCNA positive cells in ileum of IL10KO mice fed a CON (□) or GSE supplemented (■) diet. (A) Statistic data; (B) Representative image, original magnification at 200×. *: $P < 0.05$ (Mean ± SEM, n=8). The black arrows indicate brown stained PCNA positive cells. IL10KO: IL-10-deficient; WT: wild type; CON: control; GSE: grape seed extract.

Fig.4. p65 phosphorylation and protein content in ileum of IL10KO or WT mice fed a CON (□) or GSE supplemented (■) diet. (A) Representative western blot images; (B) Statistic data. Histogram bars with the same letter do not differ significantly at P = 0.05 (Mean ± SEM, n=8). IL10KO: IL-10-deficient; WT: wild type; CON: control; GSE: grape seed extract.

Fig.5. Beclin-1 and total AMPK and phosphorylated AMPK protein contents in ileum of IL10KO or WT mice fed a CON (□) or GSE supplemented (■) diet. (A) beclin-1 protein content (Top: representative western blot images; bottom: statistic data); (B) total and phosphorylated AMPK protein content (Top: representative western blot images; bottom: statistic data). Histogram bars with the same letter do not differ significantly at P = 0.05 (Mean ± SEM, n=8). IL10KO: IL-10-deficient; WT: wild type; CON: control; GSE: grape seed extract.

Fig.6. Tight junction protein content in ileum of IL10KO or WT mice fed a CON (□) or GSE supplemented (■) diet. (A) Representative western blot image; (B) Statistic data. Histogram bars with the same letter do not differ significantly at P = 0.05 (Mean ± SEM, n=8). IL10KO: IL-10-deficient; WT: wild type; CON: control; GSE: grape seed extract.

377

378

379

Figure 1

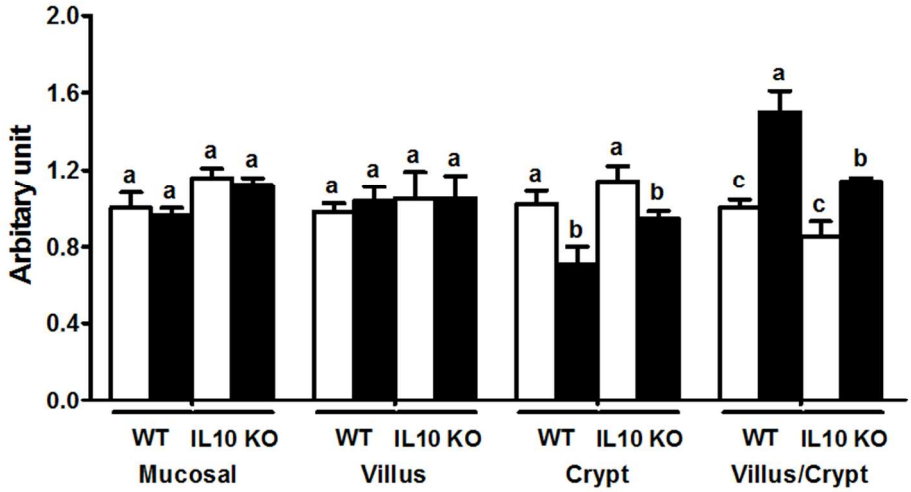

317x204mm (72 x 72 DPI)

Figure 2

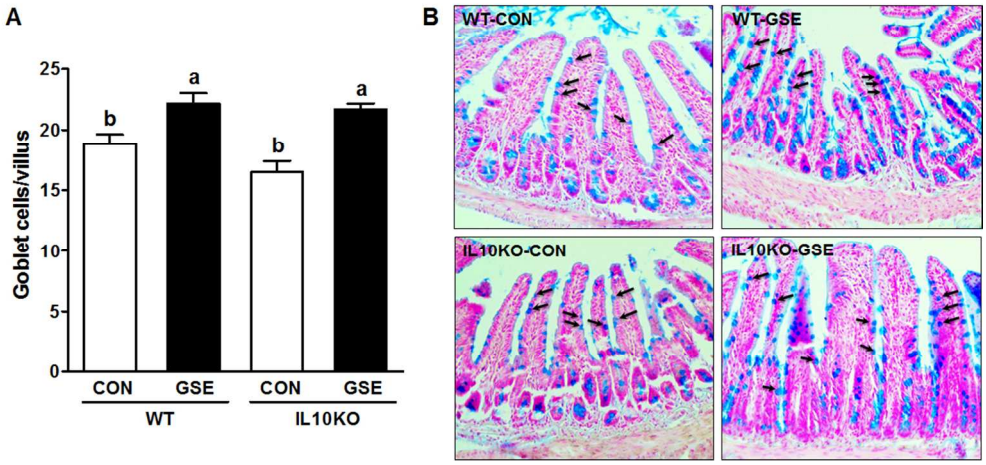

426x225mm (72 x 72 DPI)

Figure 3

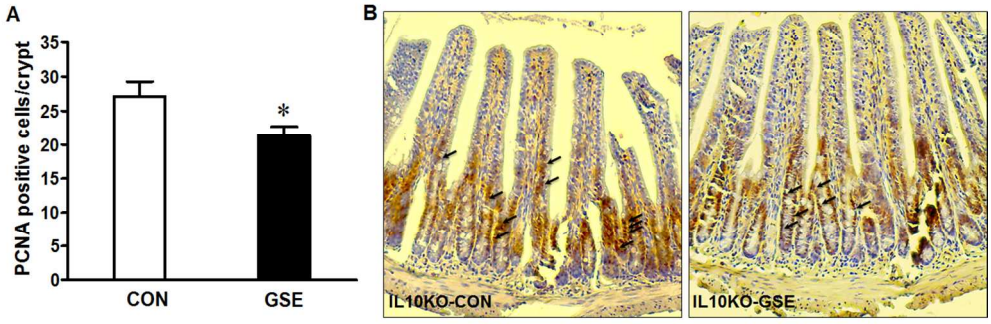

487x191mm (72 x 72 DPI)

Figure 4

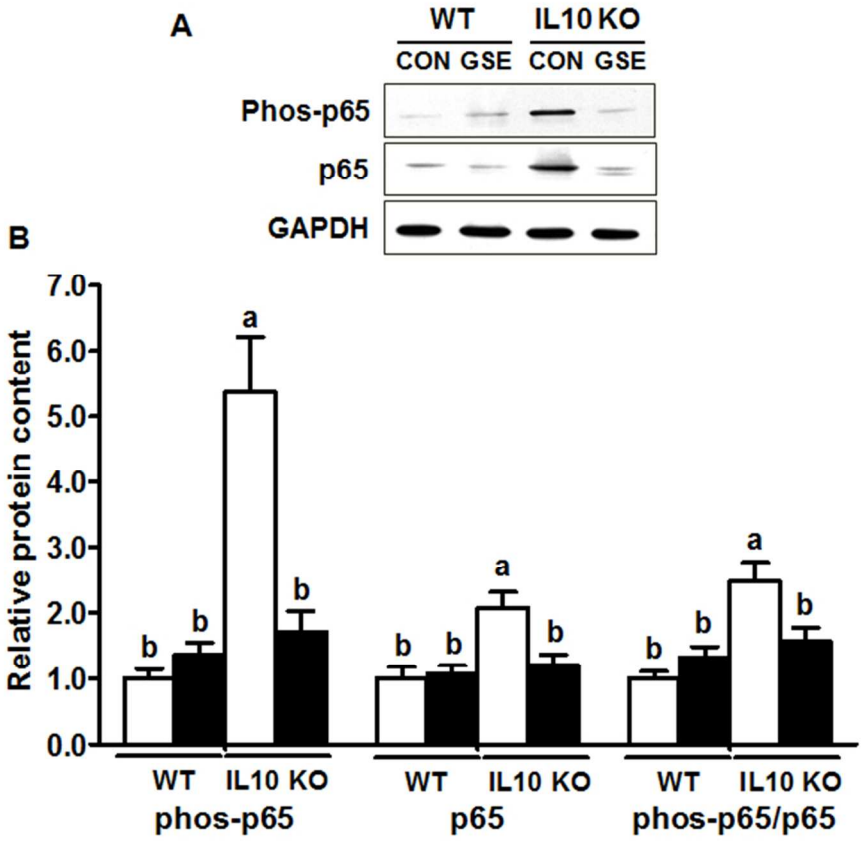

236x230mm (72 x 72 DPI)

Figure 5

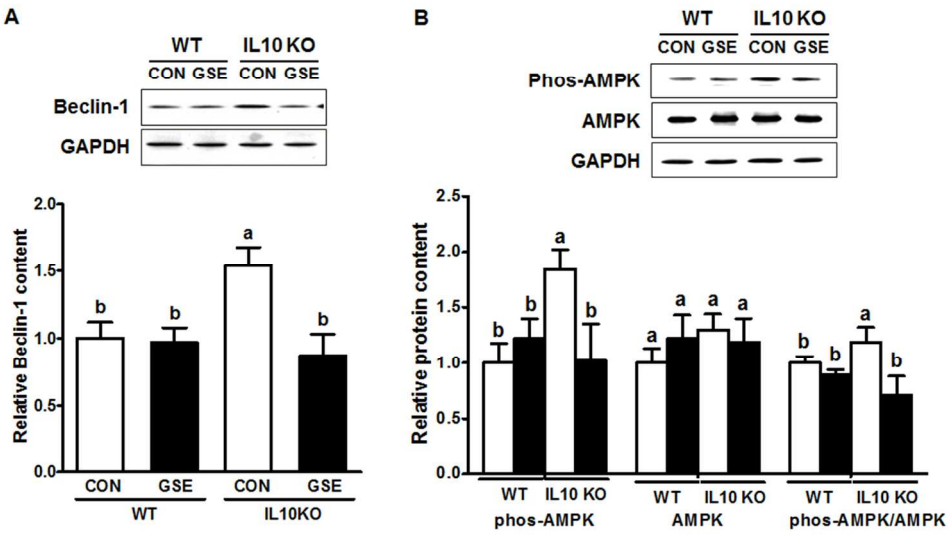

346x226mm (72 x 72 DPI)

Figure 6

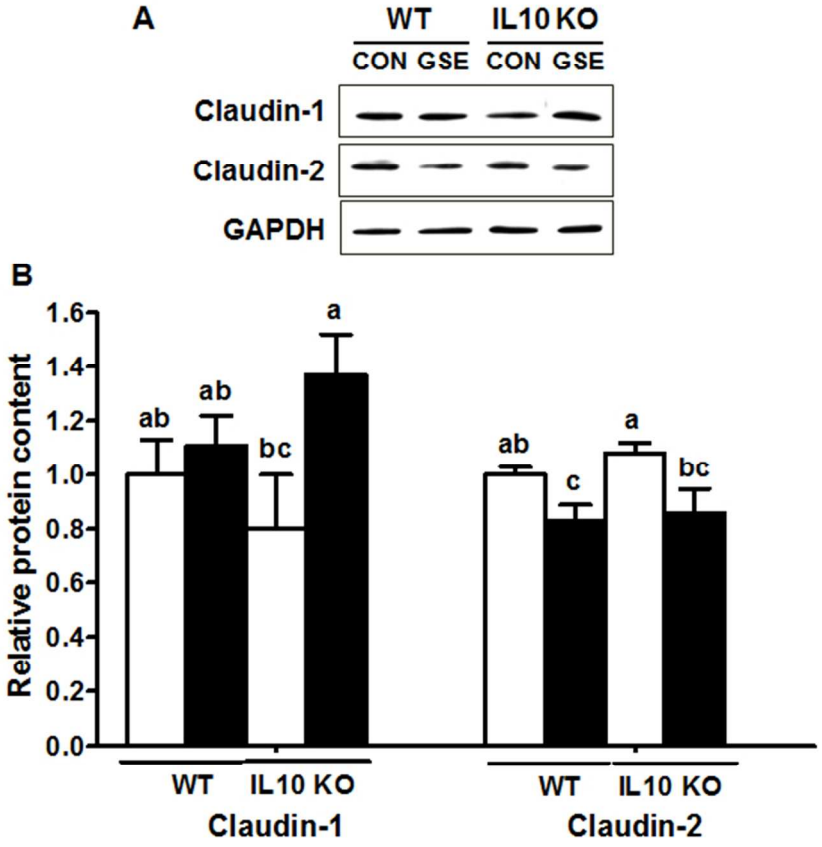

234x234mm (72 x 72 DPI)